IIIa. Nb-Ti Phase Diagram

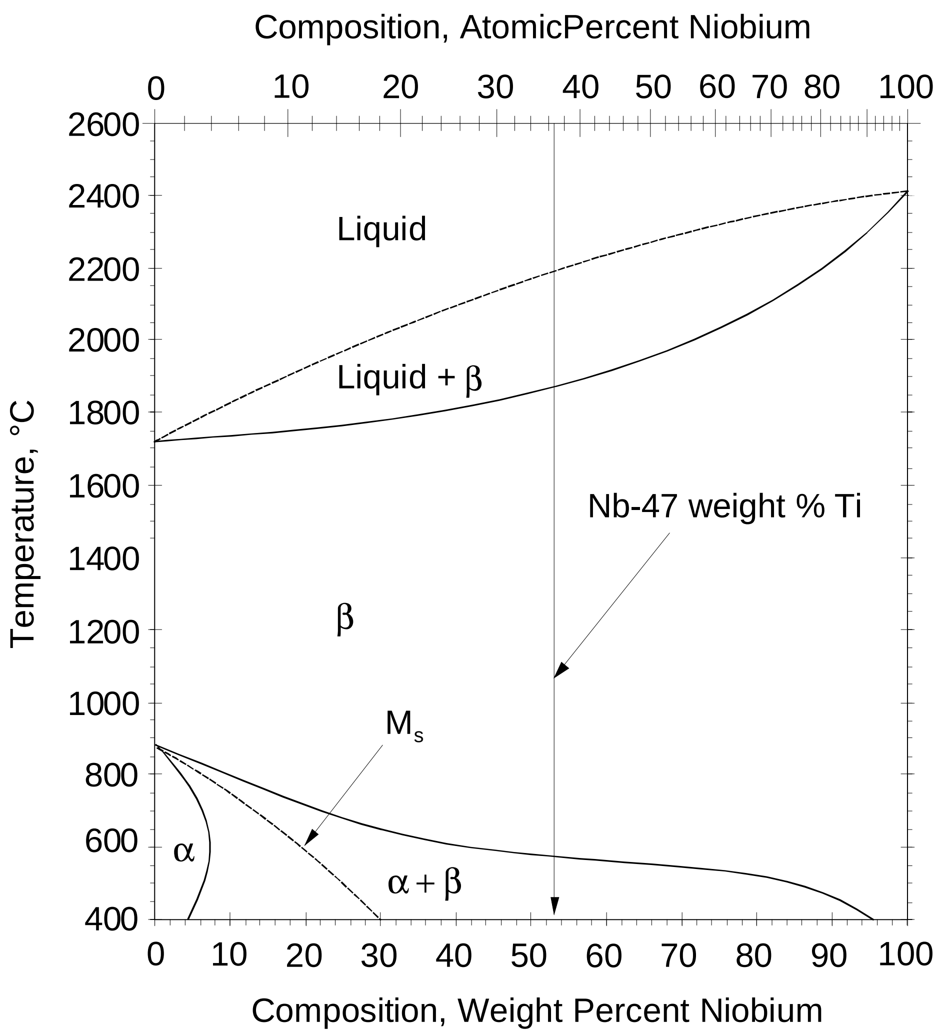

A hybrid equilibrium phase diagram for Nb-Ti combining the experimentally determined high temperature phase boundaries of Hansen et al ( ) with the calculated low temperature phase boundaries of Kaufman and Bernstein ( ) modified by Moffat and Kattner ( ). Also shown is the martensite transformation curve (M_s) of Moffat and Larbalestier ().

With thanks to Peter Lee, "*Abridged metallurgy of Ductile Alloy Superconductors,*" IEEE Encyclopeadia of Electrical Engineering

IIIb. Primary Basic Parameters

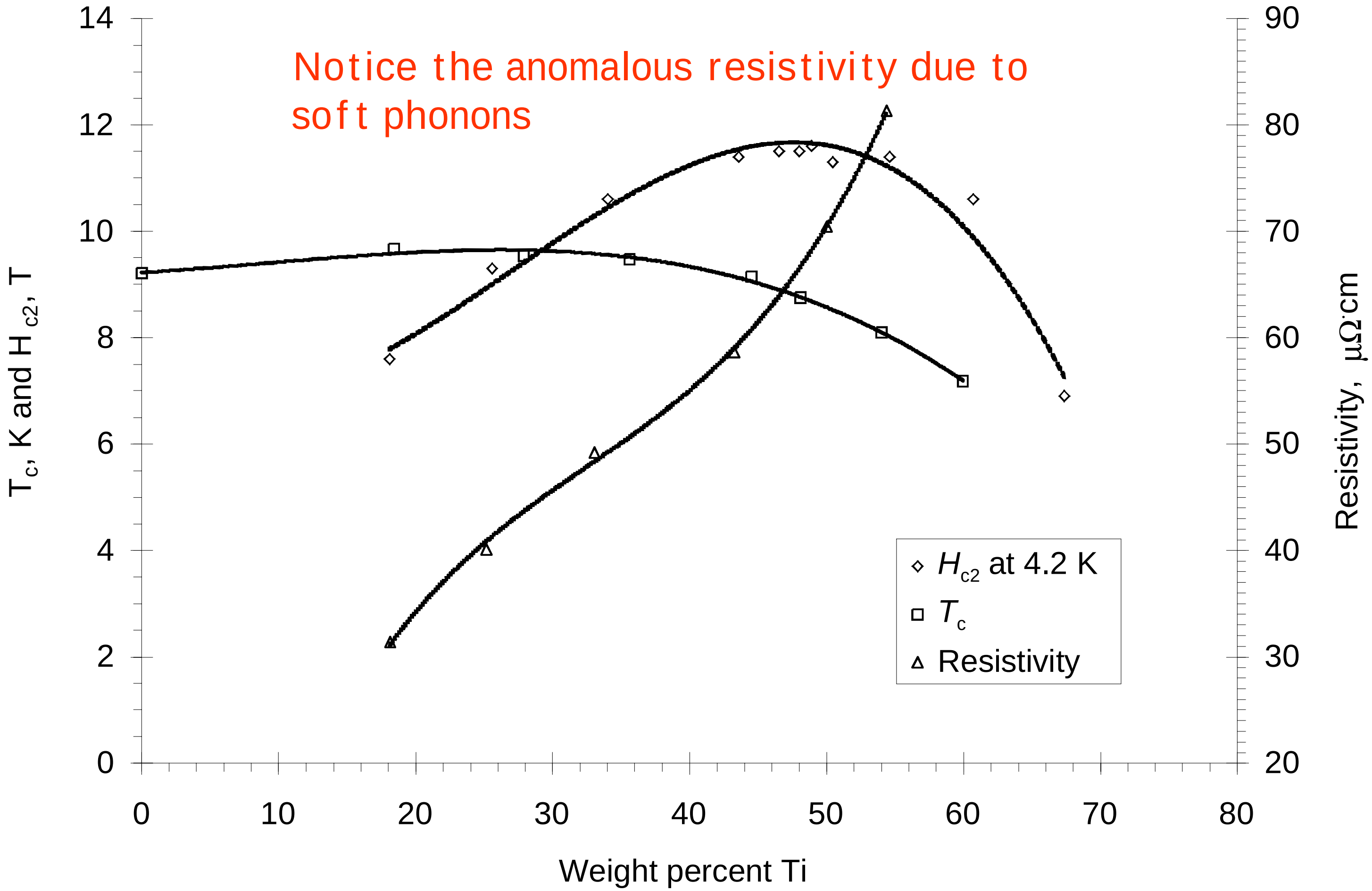

Variation in H_{c2} (4.2K data of Muller, 1987) and T_c (data of Moffat, 1985) for single phase Nb-Ti. H_{c2} is defined as the linear extrapolation of the high field pinning force (F_p) to zero (today would be defined as H*).

IIIc. Optimum nanostructure

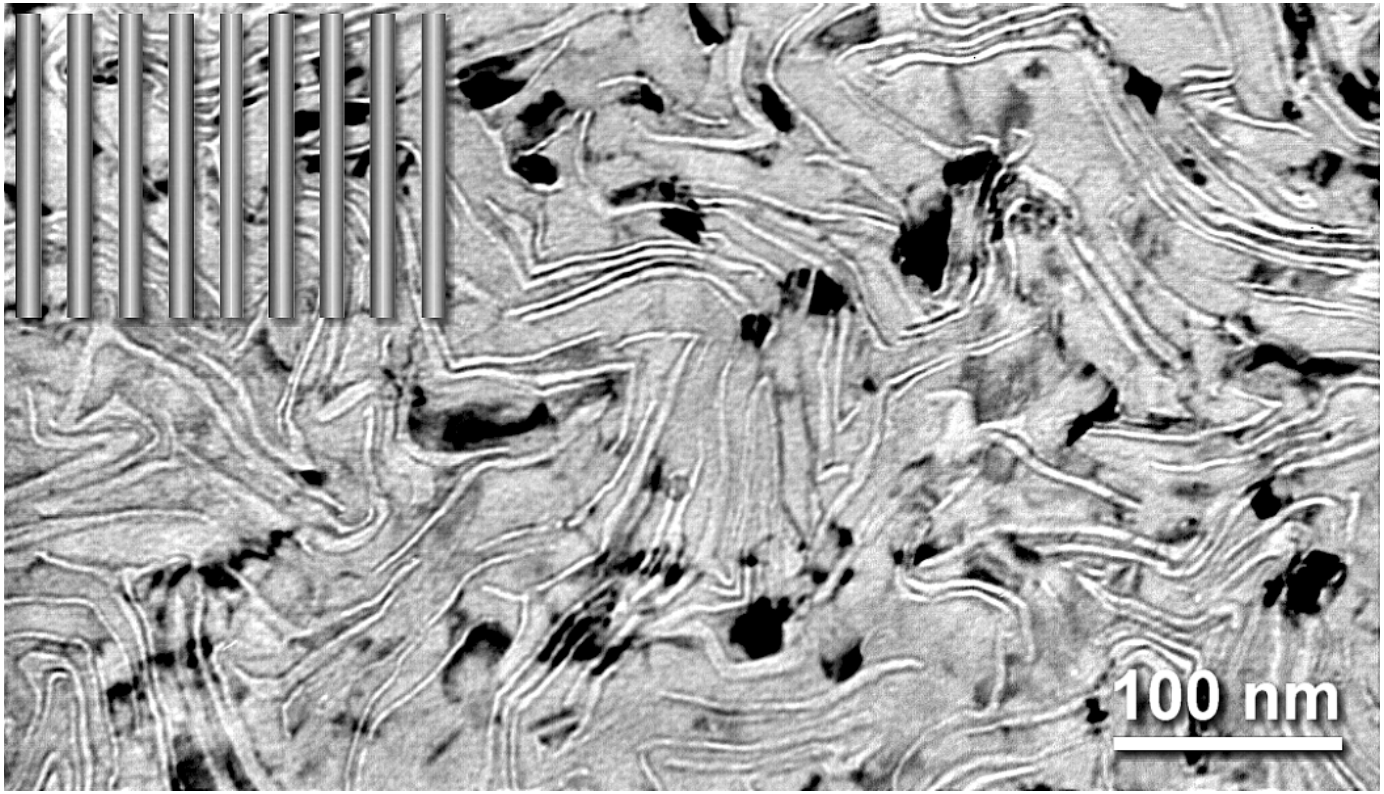

α-Ti forms ribbons 1-2 nm thick and several μm long.

Matrix is ~Nb35wt.%Ti

TEM image of very high Jc Nb-47 weight % Ti at final size in transverse cross-section reveals a densely folded array of second phase, non-superconducting α-Ti pins that closely matches the scale of the equilibrium fluxoid spacing at 5T (inset). Coherence length is 5nm, H_{c2}(4.2K) 12T.

IIId. Final size nanostructure requires macro homogeneity

Micro-chemical Ti-Nb segregation inhomogeneity revealed by etching due to wide separation of liquidus and solidus. The control of this segregation is vital as this controls the uniformity of α-Ti precipitate size and flux pinning center. Sample shown is a high homogeneity Fe doped Nb 46 weight % Ti alloy made by Teledyne Wah Chang, Albany OR.

Ingot is shown at large size. Desired final size of precipitates is 1-2 nm thick.

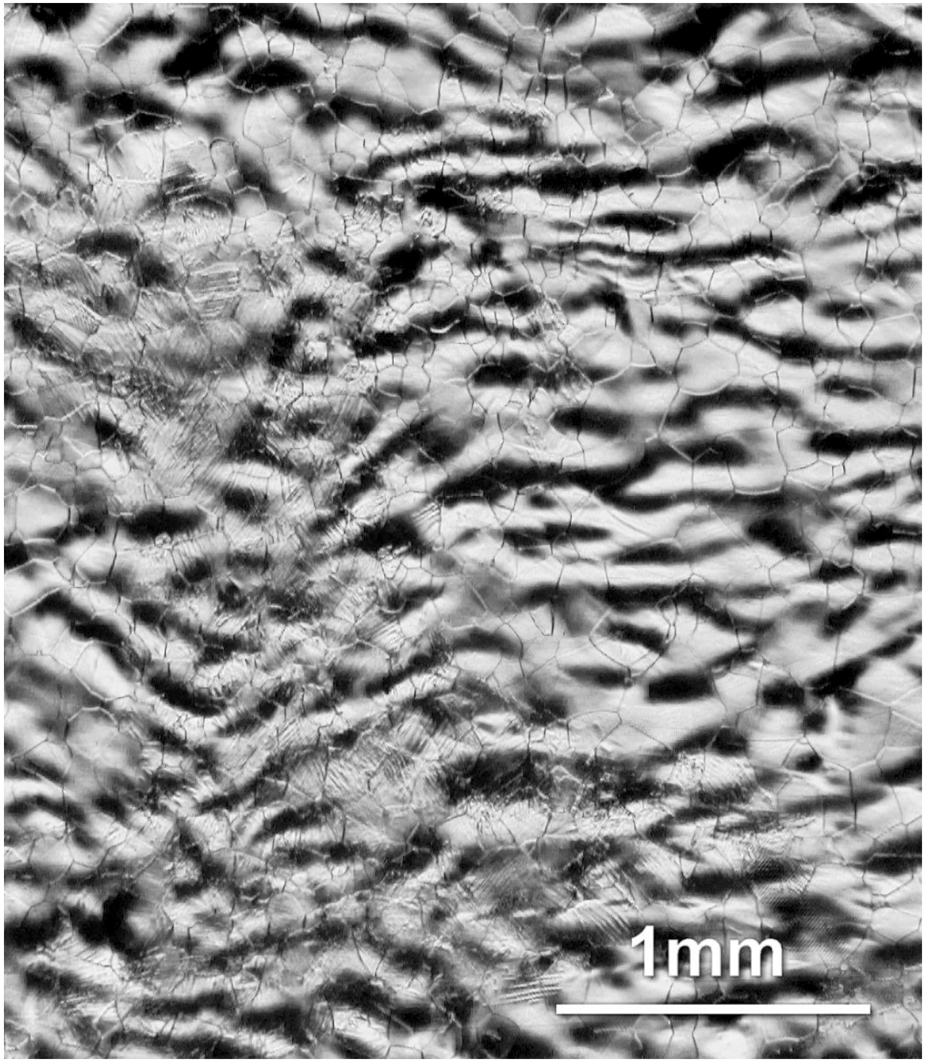

IIIe. Uniform α-Ti pinning array at last heat treatment size

High resolution back-scattered electron scanning electron microscope image of the Nb-Ti adjacent to a Nb diffusion barrier (white) after the third and final α-Ti precipitation heat treatment.

At this stage the α-Ti is ~100 nm in diameter and several times longer. A final reduction in wire diameter of 8-10x will turn the precipitates into ribbons 1-2 nm thick.

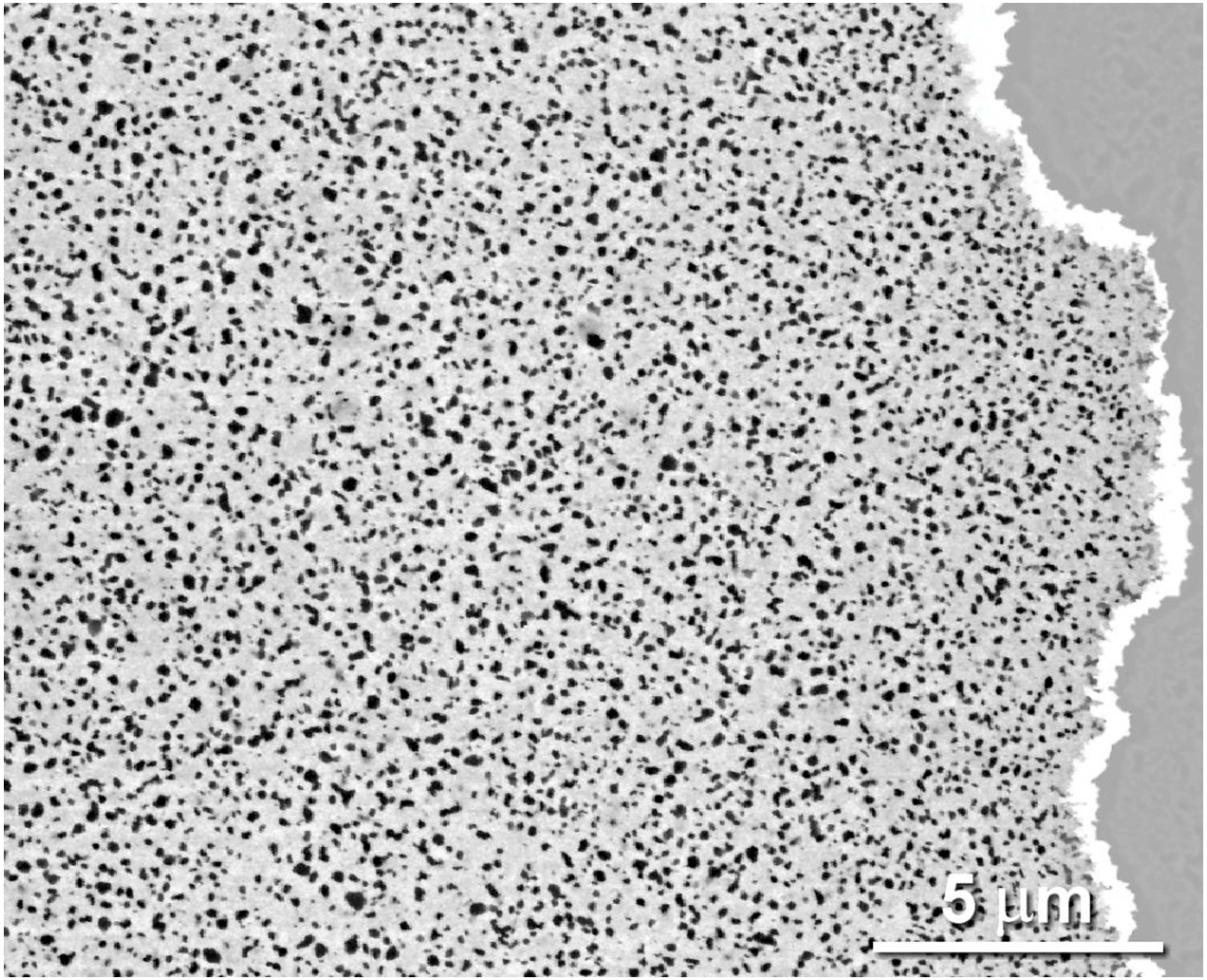

IIIf. The Fabrication Process

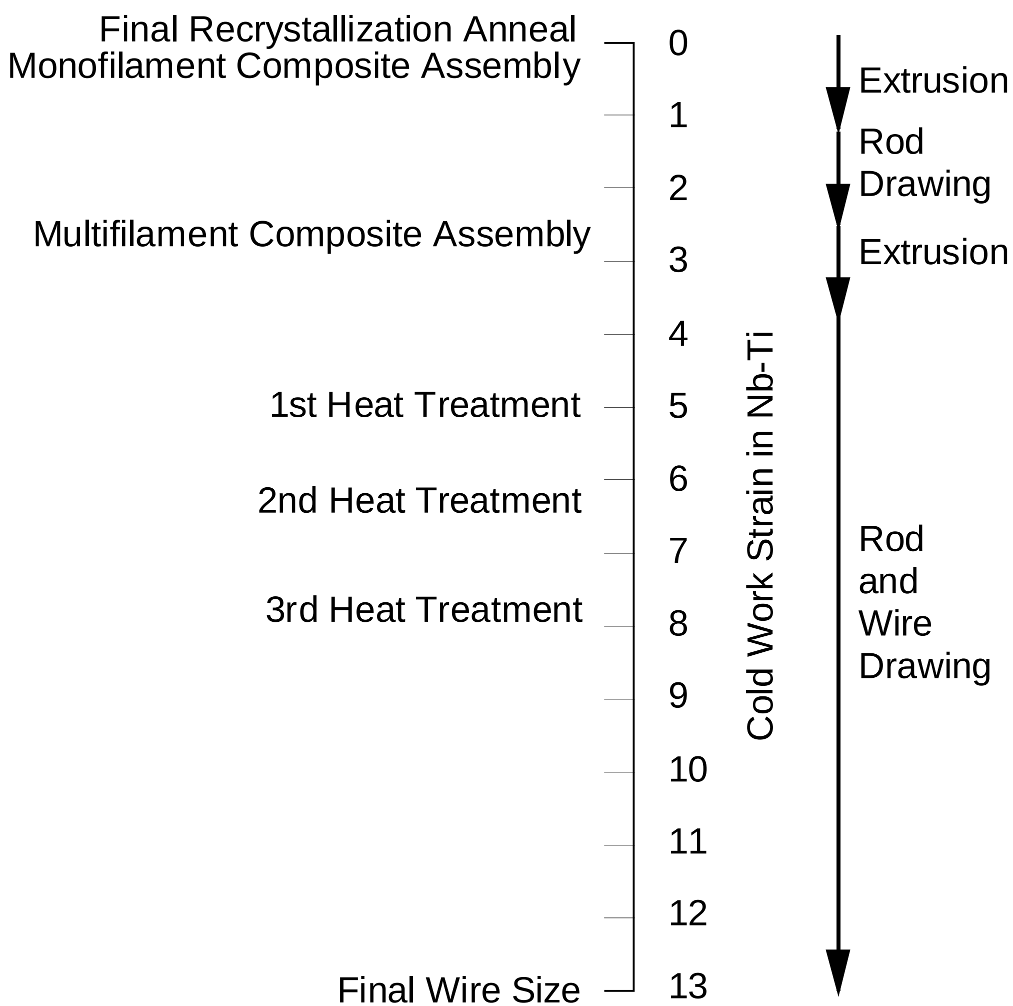

Schematic of the process for Nb-Ti superconductors in terms of cold work strain.

Strain e = 2 ln $D_{starting}/D_{final}$

300 mm diameter to 0.5-1 mm dia.

The 3 HT produce the 20vol.% of α-Ti flux pins.

The final draw thins the pins to optimum flux pinning size.

This is one of the most severe cold work manufacturing processes employed anywhere.

50,000’ lengths of wire not unusual

IIIg. Pinning centers are alpha-Ti

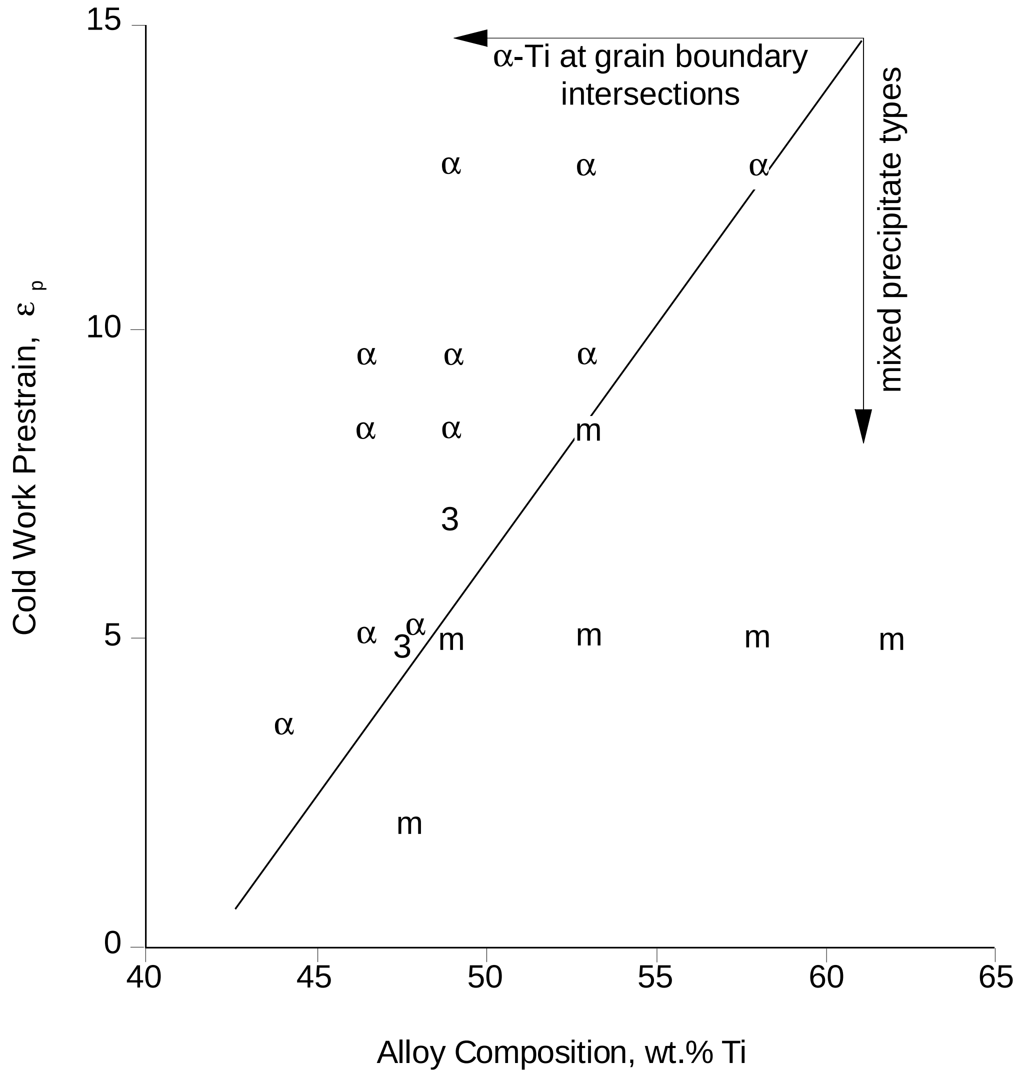

The morphology and location of precipitation in cold worked Nb-Ti alloys is determined by the amount of cold work in the microstructure. As the Ti content is increased the cold work required to produce optimum α-Ti (only at grain boundary intersections) increases. In this compilation of data (39, 40, 44) optimum precipitation is denoted by the symbol α, and mixed precipitate morphology is denoted by the letter m for heat treatment at 420 °C. The number 3 identifies where mixed mode precipitation has also been observed for 375 °C heat treatments.

IIIh. The precipitates must have the right shape

TEM image in bright field, (a) and (b), and dark field using an ω-phase reflection, (c), of a Nb-54 weight % Ti alloy after precipitation heat treatment. The heat treatment was applied at a cold work prestrain of 5 which is insufficient to avoid the deleterious ω phase and or intra-granular Widmanstaetten α-Ti forms of precipitation. In (a) the microstructure is shown in longitudinal cross-section with the drawing axis running down the page. Images (b) and (c) are of the same transverse cross-sectional area with the dark field image bringing out contrast from the ω phase.

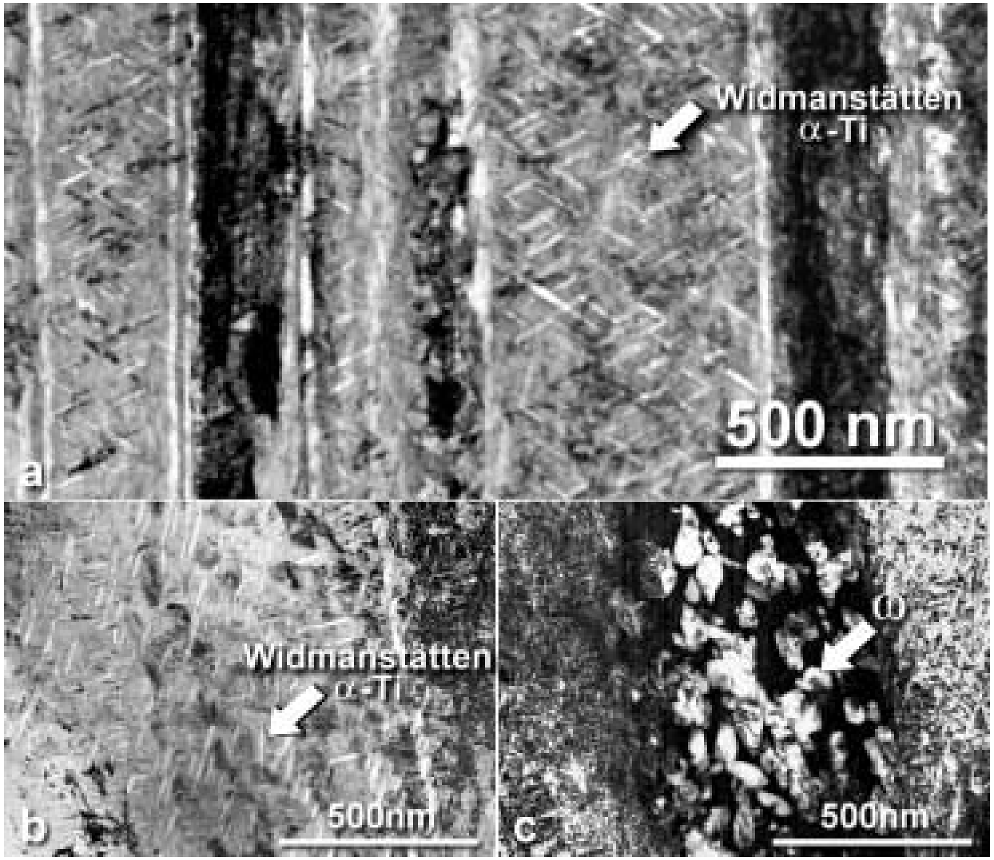

IIIi. Full summation of pinning forces

Maximum Jc increases linearly with % a-Ti precipitate from 3-25 vol. % at both 5 T and 8 T.

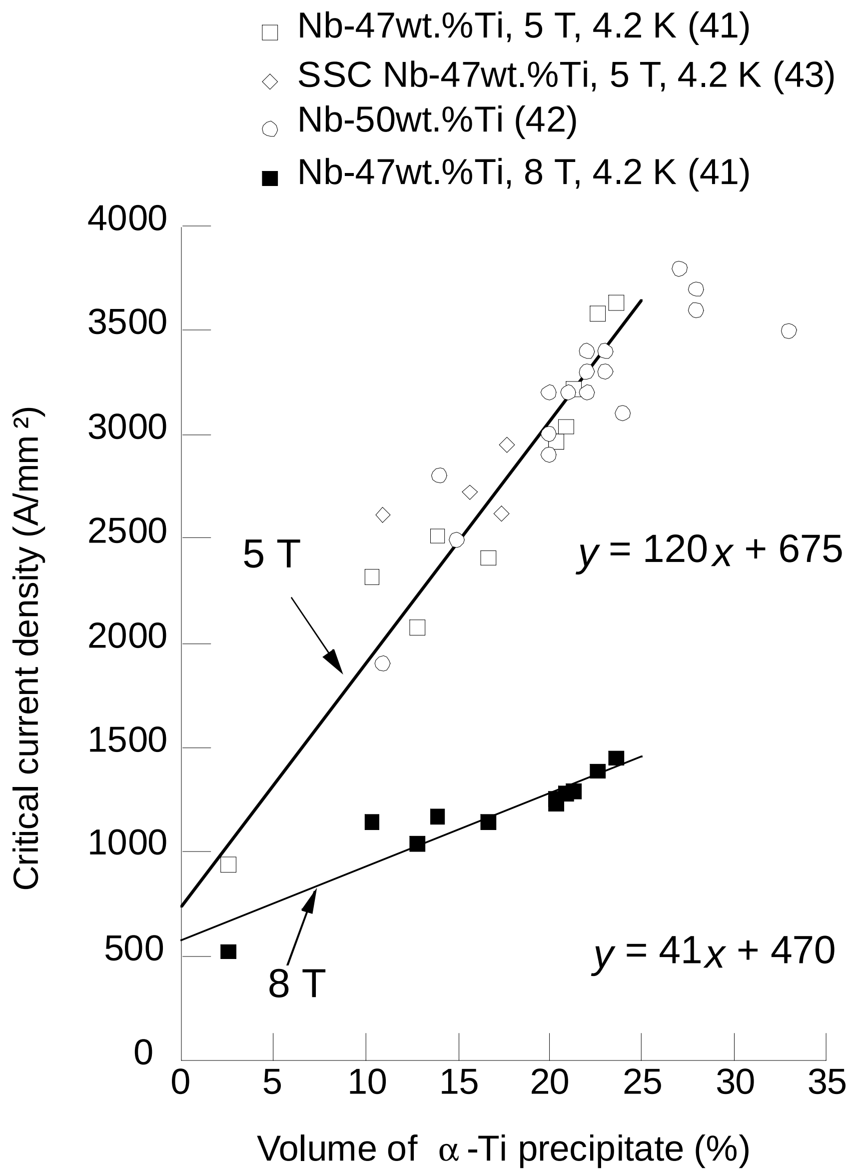

IIIj: Composition determines both pin density (and H_{c2})

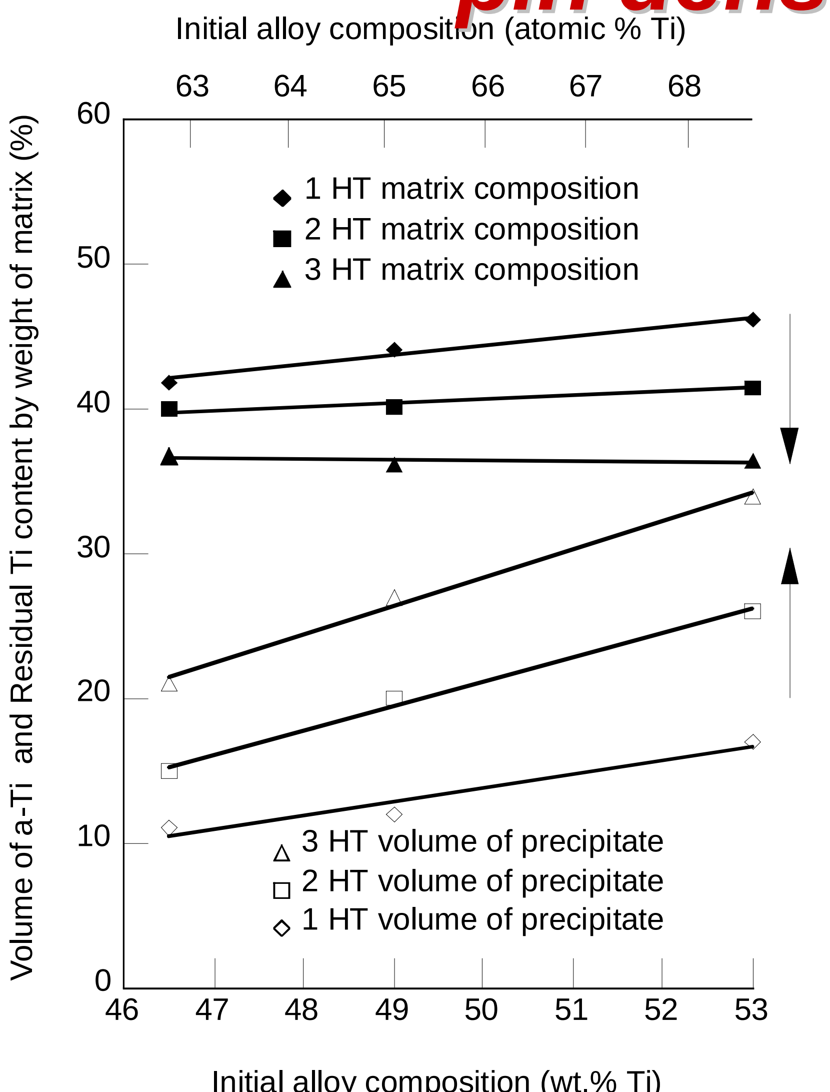

α-Ti Precipitation rate increases strongly with %Ti

- Additional heat treatments further increase the amount of precipitate.
- As additional heat treatment and strain cycles are applied, and more precipitate is produced, the residual Ti content of the β-Nb-Ti matrix drops until insufficient Ti is left to drive further precipitation.
- The average residual matrix composition is calculated assuming an α-Ti composition of Nb-3.75 atomic % Ti.

IIIk. Pinning Force Curve Shape Change

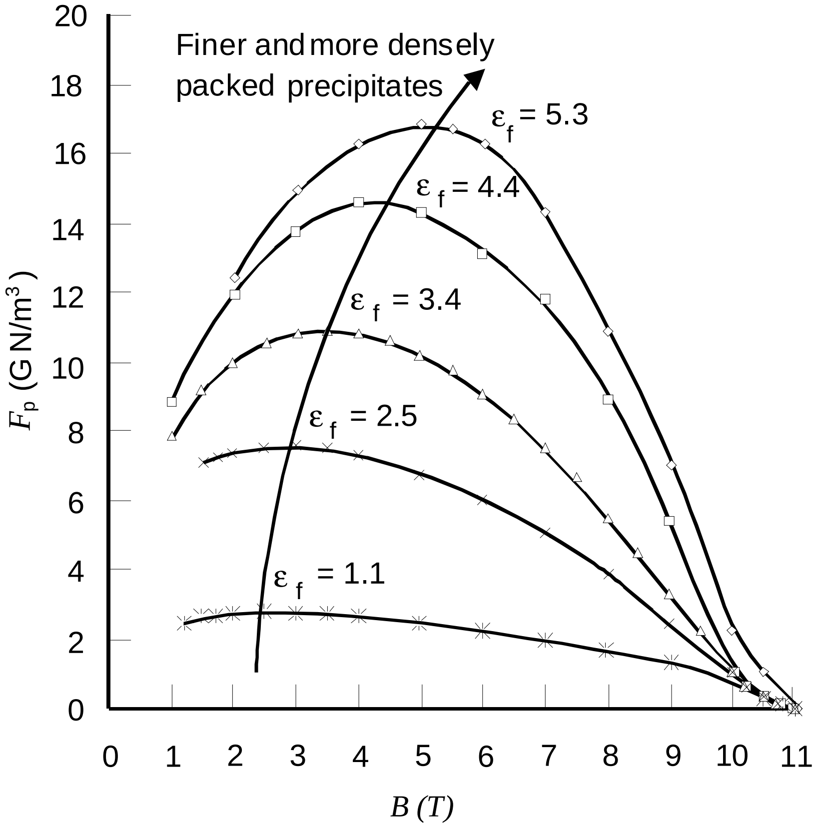

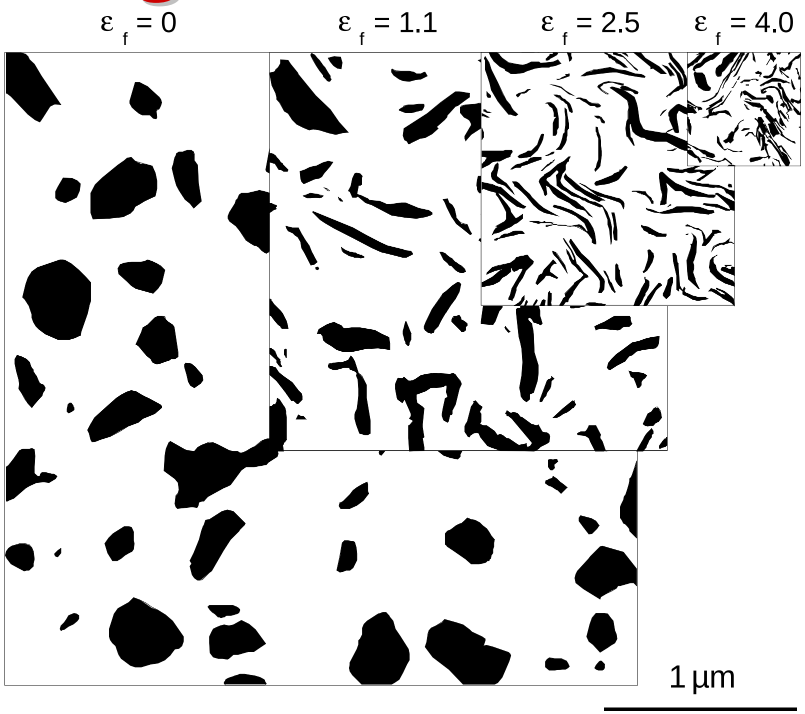

Bulk pinning force increases with drawing strain after the last heat treatment, as precipitate size and spacing are reduced to less than a coherence length in thickness. The refinement of the microstructure with increasing strain for the same strand is shown schematically in transverse cross-sections with the a-Ti precipitates in black.

III I. The Whole Composite

High quality strand at final size manufactured by IGC-AS for the Superconducting Supercollider.

An overview of the strand cross-section is superimposed on a higher magnification image showing the filament cross-sections in more detail.

Both the filament size (diameter of 6 μm) and spacing is very uniform. A Nb diffusion barrier (light-appearing ring) which prevents reaction of Cu and Ti surrounds each filament.

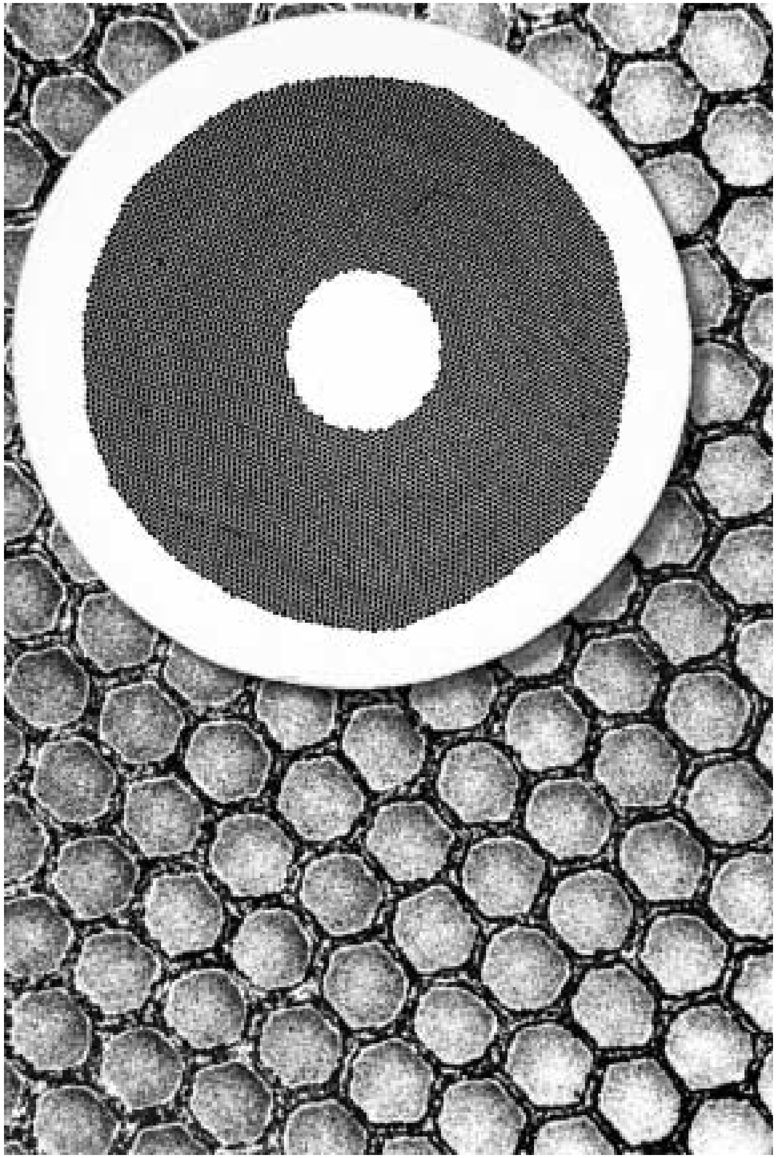

IIIm. Summary for Nb-Ti

- Mature product (~3 Ton per day for MRI, ~60,000 km per year)
  - 1/3 ton billets without breaks
- Cost ~$1/kA.m (Cu ~$20/kA.m)
- Large use for MR Imaging magnets
- Seems to be optimized now
  - Full summation of vortices against pins (15GN/m^3), ~20% of proximity-coupled pin in wire
  - But artificial pin arrays have yielded >40GN/m^3 so there is some residual uncertainty about the pinning mechanism
  - a particular point of uncertainty concerns vortex shape change as it sits on a proximity-coupled α-Ti precipitate
- Anomalous phonons due to incipient BCC⇨HCP transition are vital to developing the high H_{c2} of Nb-Ti!
  - $H_{c2} \propto \rho_n \gamma T_c$, means 12T, not 6T!